Phase Coherence upon Heating in Diblock Copolymer Films

J. Cho,*,† K. Shin,*,‡ K. S. Cho,§ Y.-S. Seo,|| S. K. Satija,⊥ D. Y. Ryu,⊗ and J. K. Kim○

Department of Polymer Science and Engineering, Dankook University and Hyperstructured Organic Materials Research Center, San 44-1, Jukjeon-dong, Suji-gu, Yongin-si, Gyeonggi-do 448-701, Korea, Department of Chemistry and Program of Integrated Biotechnology, Sogang University, Sinsu-dong, Mapo-gu, Seoul 121-742, Korea, Department of Polymer Science and Engineering, Kyungpook National University, 1370, Sangyuk-dong, Bukgu, Daeku 702-701, Korea, Department of Nano Science and Technology, Sejong University, Gunja-dong, Gwangjin-gu, Seoul 143-747, Korea, National Institute of Standards and Technology, 100 Bureau Drive, Stop 1070, Gaithersburg, Maryland 20899-1070, Department of Chemical Engineering, Yonsei University, 134 Sinchon-dong, Seodaemun-gu, Seoul 120-749, Korea, and National Creative Research Initiative for Block Copolymer Self Assembly, Department of Chemical Engineering and Polymer Research Institute, Pohang University of Science and Technology, Kyungpuk, 790-784, Korea

Received July 18, 2007; Revised Manuscript Received October 31, 2007

ABSTRACT: Phase coherence behavior in thin films of a diblock copolymer that exhibits microphase separation upon heating in the bulk has been analyzed through a proper mean-field free energy functional based on a compressible random-phase approximation theory. Phase coherent profiles at equilibrium and their decay lengths were obtained analytically for those copolymer films. Taking deuterated polystyrene-*b*-poly(*n*-propyl methacrylate) as a model system, molecular parameters characterizing the copolymer were shown to yield the growing tendency of surface segregated or phase coherent profiles upon heating. Neutron reflectivity measurements were performed for the copolymer films to be compared with theory. Phase coherence prior to bulk ordering temperatures and subsequent decay lengths observed for the given system were shown to be in agreement with theory.

Introduction

Phase separation behaviors of melts and thin films of block copolymers have drawn tremendous interest in the polymer community. Block copolymers exhibit nanoscale self-assembly behavior to form microscopically ordered structures called microphases. Most block copolymers have been known to exhibit a microphase separation from a disordered state to an ordered state upon cooling, which is referred to as the upper order−disorder transition (UODT). The unfavorable interactions between dissimilar monomers comprising a given block copolymer are considered to be the cause for such behavior.[1−3] There have been in recent decades extensive theoretical developments including Leibler's Landau approach[4] to analyze the microphase separation behavior and transitions between equilibrium microstructures for molten block copolymers or systems containing block copolymers in the weak to strong segregation regime.[1,4,5] There have been also numerous publications regarding the phase behavior of block copolymer films.[6] Among them, surface ordering or phase coherence phenomena[7,8] were investigated first by Fredrickson[9] and later by Tang and Freed[10] in the weak segregation regime. More thorough self-consistent field calculations, particle-based and field-theoretic simulation studies have appeared in the polymer literature to understand complicated nanopatterns of the copolymer melts and films.[1,6,11,12] Very recently, Angerman et al. developed an analytical Landau free energy density for thin block copolymer films that is amenable to capture a global overview of nanopatterned films in various ways.[13] It is a central concept in all of the works that a composite parameter $N\chi_F$, where N and χ_F are the copolymer chain size and Flory's interaction parameter, respectively, forms a relevant parameter to describe the phase behavior of block copolymer systems.

The theories mentioned above are based on the common assumption of system incompressibility. However, there have been numerous recent findings that strongly address a clear need for finite compressibility to interpret the compressible nature and the pressure effects of block copolymers. The relevant findings include ordering upon heating, which is referred to as lower disorder−order transition (LDOT) phenomena, in styrenic block copolymer melts and films,[14−17] baroplastic copolymers to utilize pressure-induced flow,[18−23] and loop-forming block copolymers.[20,23−26] Prior to the discovery of loop forming block copolymers, the LDOT and baroplastic character of styrenic block copolymers have been attributed to the difference in monomer structures by Freed and co-workers in their lattice cluster model[27] or to the difference in pure component properties by Ruzette and Mayes in a simple phenomelogical model.[28,29] However, a unified view of the LDOT, loop, and baroplasticity in those styrenic block copolymers has been provided in a recent series of works by one of the present authors on a compressible random-phase approximation (RPA) theory.[30−34] Finite compressibility was incorporated into the theory through effective RPA interactions, which is obtained from a molecular equation-of-state model by Cho and Sanchez (C−S).[35,36] The χ_F was reinterpreted as $\chi_F = \chi_{app} + \chi_{comp}$, where χ_{app} is the density dependent dimensionless exchange energy and χ_{comp} represents compressibility difference between constituent blocks.

LDOT or baroplastic block copolymers can offer new types of sensor materials with high-temperature or pressure sensitivity.

* To whom correspondence should be addressed. E-mail: jhcho@dku.edu (J.C.), kwshin@sogang.ac.kr (K.S.).
† Dankook University, and Hyperstructured Organic Materials Research Center.
‡ Sogang University.
§ Kyungpook National University.
|| Sejong University.
⊥ National Institute of Standards and Technology.
⊗ Yonsei University.
○ Pohang University of Science and Technology.

10.1021/ma071604r CCC: $40.75
Published on Web 01/16/2008

It is clear that the incompressible approaches are incapable of predicting or interpreting phase coherence in those copolymer films with selective surface fields. More detailed molecular information is needed to be put into χ_F for such purposes. Here, it is our objective to suggest a theoretical framework to solve the problem at hand. We employ an effective Landau free energy density from our compressible RPA theory. The free energy density is manipulated by using the Ohta−Kawasaki-type approach[5,9] to obtain a real-space free energy functional, and surface−monomer interactions are considered to act as an external field. Minimization of the free energy functional yields the Euler−Lagrange equation, which is analytically solved in a linearized fashion for the films of symmetric block copolymers in the weak segregation regime. Taking LDOT-type baroplastic diblock copolymer from deuterated polystyrene and poly(*n*-propyl methacrylate) as a model system, it is shown that requisite molecular parameters characterizing block components readily yield the phase coherence behavior of the copolymer films, which is in agreement with neutron reflectivity results. Furthermore, the concept in the present approach to include molecular information can be implemented into other phenomenological theories such as the Landau theory by Angerman et al.[13] or a more elaborate self-consistent field theory.

Theory

Let us consider A−B diblock copolymers of chain size N with N_i monomers of i-type. Copolymer chains are assumed as perturbed hard sphere chains of uniform size σ in a continuum. The nonbonded perturbed i,j-interactions are characterized by ϵ_{ij}. A hard-core volume fraction of i-monomers on the copolymer chains is defined by $\phi_i \equiv N_i/N$. We denote η_f as the fraction of free volume in the system, and $\eta = 1 - \eta_f$ as the total dimensionless density of all the monomers present. In a Landau analysis, the difference δF in free energies between ordered and disordered states is expanded as a power series in the two order parameters, $\bar{\psi}_1(\vec{r})$ and $\bar{\psi}_2(\vec{r})$, where the former is given from the thermal average of the differences between the local density $\eta_i(\vec{r})$ and the global density $\eta\phi_i$ of i-monomers as $\bar{\psi}_1(\vec{r}) \equiv \langle \eta_A(\vec{r})/\eta - \phi_A\rangle/2 - \langle \eta_B(\vec{r})/\eta - \phi_B\rangle/2$, and the latter from that between the local free volume fraction $\eta_f(\vec{r})$ and the global one η_f as $\bar{\psi}_2(\vec{r}) \equiv -\langle \eta_f(\vec{r}) - \eta_f\rangle$. The free energy can then be written as $\beta\delta F = \sum_{m=2}^{\infty}(1/m!)\int d\vec{q}_1 ... d\vec{q}_m \bar{\Gamma}^m_{i_1,..i_m}\bar{\psi}_{i_1}...\bar{\psi}_{i_m}$ with the Fourier-transformed ψ_i, where $\bar{\Gamma}^m$ is the proper mth-order vertex function. The Fourier space variable $\vec{q}$ physically means the scattering vector, whose magnitude is wave number. This Landau expansion is first approximated as the sums containing only the most important contributions from the fastest growing characteristic waves. After the minimization procedure is undertaken for $\bar{\psi}_2$, the Landau free energy expansion can then be cast back into the continuum space expressions as a series in only $\bar{\psi}_1$ up to the quartic-order now with the effective vertex coefficients.[31] Mathematically stated,

$$\beta\delta F = \frac{1}{2}\int d\vec{q}_1 [\bar{\Gamma}_{11} - \bar{\Gamma}_{12}^2/\bar{\Gamma}_{22}]\bar{\Psi}_1(\vec{q}_1)\bar{\Psi}_1(-\vec{q}_1) + \frac{1}{3!}\int d\vec{q}_1 d\vec{q}_2 [\bar{\Gamma}_{111} - \Delta]\bar{\Psi}_1(\vec{q}_1)\bar{\Psi}_1(\vec{q}_2)\bar{\Psi}_1(-\vec{q}_1 - \vec{q}_2) + \frac{1}{4!}\int d\vec{q}_1 d\vec{q}_2 d\vec{q}_3 \bar{\Gamma}_{1111}\bar{\Psi}_1(\vec{q}_1)\bar{\Psi}_1(\vec{q}_2)\bar{\Psi}_1(\vec{q}_3)\bar{\Psi}_1(-\vec{q}_1 - \vec{q}_2 - \vec{q}_3) \quad (1A)$$

where Δ in eq 1A is written explicitly as

$$\Delta = [\bar{\Gamma}_{112} + \bar{\Gamma}_{121} + \bar{\Gamma}_{211}]_{q_1,q_2,-q_1-q_2} \times [|\bar{\Gamma}_{12}|/\bar{\Gamma}_{22}]_{q_1,-q_1} \quad (1B)$$

In eq 1B, $\bar{\Gamma}_{112}$ and the other two are evaluated for the three wave vectors forming an equilateral triangle, and thus Δ is vanishing for lamellae. It is to be seen in the following paragraph that $\bar{\Gamma}_{12}$ and $\bar{\Gamma}_{22}$ are directly related to proper phenomenological terms. The two contributions, $\bar{\Gamma}_{12}^2/\bar{\Gamma}_{22}$ and Δ, are the main corrections to the free energy due to the compressibility difference between block components.

In eq 1, $\bar{\Gamma}_{11}(q^*)/\eta = 2\chi_s - 2\chi_{app}$ when evaluated at the ground state q^*, where $2\chi_s$ is the combination of the pair correlation functions S^0_{ij}'s of noninteracting Gaussian A−B copolymers as $2\chi_s = \sum\eta S^0_{ij}(q^*)/\det[S^0_{ij}(q^*)]$. The symbol χ_{app} denotes the density-dependent dimensionless exchange energy as $\chi_{app} \equiv (\beta h_z \Delta\epsilon/2)|u(\eta)|$, where $\Delta\epsilon \equiv [\epsilon_{11} + \epsilon_{22} - 2\epsilon_{12}]$ is the exchange energy and $u(\eta)$ describes the density dependence of nonbonded perturbed interactions in the C−S model[35,36] as $u(\eta) = 4[(\gamma/C)^4\eta^4 - (\gamma/C)^2\eta^2]$ with $\gamma = 1/\sqrt{2}$ and $C = \pi/6$. The symbol h_z implies the number of nonbonded nearest neighbors, where $h_z \approx 10$ in dense polymeric liquids. In our previous works,[31,32] χ_{comp} was introduced as $\chi_{comp} \equiv \bar{\Gamma}_{12}^2/2\eta\bar{\Gamma}_{22}$ and then the effective Flory interaction parameter χ_F as $\chi_F \equiv \chi_{app} + \chi_{comp}$. It was recently identified that for a symmetric copolymer in the long chain limit $\eta\bar{\Gamma}_{12} = \beta\upsilon^*(\partial P/\partial\phi)_{T,\upsilon}$, $\eta^2\bar{\Gamma}_{22} \approx \beta B_T\upsilon^*$, and then $\chi_{comp} \approx \upsilon^*(\partial P/\partial\phi)^2/\eta B_T$, where υ^* is the volume of one monomer.[34] The $(\partial P/\partial\phi)_{T,\upsilon}$ represents the disparity in equation-of-state properties between constituents and B_T, the isothermal bulk modulus. By the Maxwell relations, it can also be shown that $\bar{\Gamma}_{12}/\bar{\Gamma}_{22} \approx -(\partial\eta/\partial\phi_1)_{T,P}$. Therefore, the contributions pertinent to compressible systems appearing in quadratic and cubic terms are converted to bulk thermodynamic quantities. If $\bar{\Gamma}_{12}$ or $(\partial P/\partial\phi)_{T,\upsilon}$ is absent, χ_{comp} and Δ disappear, and $\delta F/\eta$ in eq 1 becomes mathematically identical to the free energy of Leibler, except that the density dependent χ_{app} is used instead.[31]

To obtain a real-space free energy functional for copolymer films, the free energy expression in eq 1 is further approximated in an Ohta−Kawasaki-type approach.[5,9] The effective second-order vertex function is treated as $N[\bar{\Gamma}_{11} - \bar{\Gamma}_{12}^2/\bar{\Gamma}_{22}]/\eta \approx A/q^2 + Bq^2 - \bar{\chi}$, where A and B are, respectively, given as $A = {}^3/_2\phi^2(1-\phi)^2R_g^2$ and $B = (R_g^2/2\phi)(1-\phi)$ with the gyration radius R_g. The $\bar{\chi}$ in this expression is given as $\bar{\chi} \equiv 2N\chi_F(q^*) - 2N\chi_s + \sqrt{3}/[\phi(1-\phi)]^{3/2}$. For the simplicity of the analysis, we assume a one-dimensional lamellar ordering of the symmetric copolymer, which removes the effective third-order vertex function term in eq 1. The free energy functional in real space for the films with thickness LR_g can be shown to possess a term with the Green function $G(x-x')$ (from A/q^2) and the square gradient term (from Bq^2). The surface interactions for the films are treated as the external field term, $-\int_{-L/2}^{L/2} \beta H_{\mp}\,\delta(x \pm L/2)\bar{\psi}_1(x)$, added into the free energy functional, where $H_{\mp}$ describes the extremely short-ranged surface−monomer interactions acting at the position $x = \pm L/2$. The standard minimization of the obtained free energy functional yields the Euler−Lagrange equation. It needs to be noted that a Lagrange multiplier θ for the material balance $(\int\bar{\psi}_1(\mathbf{r})\, d^3\mathbf{r} = 0)$ is required in the formulated Euler−Lagrange equation. The boundary conditions are then as follows: $-\beta H_{\pm} \pm B\, d\bar{\psi}_1/dx = 0$ at $x = \pm L/2$. We are interested in the phase coherence transition prior to bulk ODT, so that by adopting the simplest form of the Green function as $G(x-x') = x - x'$ if $x > x'$, and zero otherwise, the linearized solution of the given Euler−Lagrange equation can be obtained as[6,9]

$$\bar{\psi}_1(x) = e^{x/\xi}(A_{c+}\cos\Omega x + A_{s+}\sin\Omega x) + e^{-x/\xi}(A_{c-}\cos\Omega x + A_{s-}\sin\Omega x) \quad (2)$$

Table 1. Characteristics of Deuterated Polystyrene-*b*-poly(*n*-propyl methacrylates) (D-PS−PPrMA)

sample	M_n	PDI	ϕ_{D-PS}	R_g (Å)[a]	LDOT (°C)
H	135 000	1.02	0.50	92	193−195[b]
M	119 600	1.02	0.51	87	225[b]
L	75 300	1.02	0.53	69	disordered

[a] R_g were approximated by $6.7\sqrt{(N/6)}$ (in Å). [b] Determined by rheometry and small-angle neutron scattering. See ref 40.

where a transformation of $x + L/2 \rightarrow x$ has been done in eq 2. The ξ and Ω are, respectively, the decay length and the wave number of the developed profile, which are defined, respectively, as

$$\xi = \sqrt{\frac{4B/\bar{\chi}_S}{1-(\bar{\chi}/\bar{\chi}_S)}}; \quad \Omega = \sqrt{\frac{\bar{\chi}_S}{4B}}\sqrt{1+\frac{\bar{\chi}}{\bar{\chi}_S}} \tag{3}$$

with $\bar{\chi}_S = 2\sqrt{AB}$. The four coefficients of eq 2 can be given from $\bar{\psi}_1(0)$, $\bar{\psi}_1'(0)$, and θ, as is written in the Appendix. The composition profile given in eq 2 along with the necessary coefficients and the decay length are now ready to be evaluated for phase coherent block copolymer films.

Experimental Procedures

Materials and Sample Preparation. Deuterated polystyrene-*block*-poly(*n*-propyl methacrylates) (D-PS−PPrMA) with symmetric composition were synthesized by the sequential, anionic polymerization of deuterated styrene and *n*-propyl methacrylate in tetrahydrofuran at −78 °C in the presence of LiCl under purified Ar using *sec*-BuLi as an initiator. The characteristics of the samples produced in such a way are listed in Table 1. Prior to spin-coating, the silicon wafers (5 mm thick, 76 mm diameter) were placed in a HF buffered solution to remove the native oxide layer and then placed into a UV/ozone cleaner for 20 min to reform the oxide surface. By this method, typical 20 Å thick oxide layers were expected as previously reported.[37] A series of the diblock copolymers were spin cast from toluene solutions on the silicon wafers. The polymer radius of gyration (R_g) in Table 1 is estimated by $R_g = 6.7$ Å$(N_e/6)^{1/2}$ where N_e is a sum of the polymerization indices of two blocks. The film thickness was controlled to be $\sim$ 1200 Å by varying polymer mass fractions in toluene solutions. The films were then preannealed for 5 h in vacuum at 90 °C to evaporate any residual solvents that remained in the films.

Neutron Reflectivity. Specular reflectivity measurements were performed on the NG7 neutron reflection spectrometer at the NIST Center for Neutron Research at the National Institute of Standards and Technology with a wavelength λ of 4.76 Å and a $\Delta q/q$ of 0.04. In order to monitor in situ phase transition phenomena as a function of temperature, a specially designed high-temperature cell was used; the sample is secured against a large copper heating block, centered inside an aluminum enclosure. The aluminum sidewalls allow the neutron beam to pass through with single-crystal windows. A turbo pump is attached to the cell, yielding a pressure of $P \sim 10^{-6}$ mbar, while a top lid is screwed on securely, maintaining a high vacuum condition in order to reduce background scattering and protect the sample from oxidation at high temperature. A thermocouple reads the temperature of the copper heating block, and a feedback loop ensures that the sample is held at the proper temperature. During 4 h of a typical neutron reflectivity scan, the temperature was simultaneously recorded and deviations from the set point were less than ± 0.2 °C. The operating temperature range was from room temperature to 300 °C. The annealing time before the measurements was set to 30 min.

For the specular reflection, the scattering vector, $q = k_f - k_i$, is only in the *z*-direction which is normal to the interface. Since $q_x = q_y = 0$, it is given by $q_z = (4\pi/\lambda)\sin\alpha_i$, where α_i is the incident angle. By the Born approximation at $q_z > 4q_c$, where q_c is the critical angle for total reflection, the reflectivity, $R(q_z)$, is expressed essentially as

$$R(q_z) \propto R_F\left|\int \frac{\mathrm{dSLD}(z)}{\mathrm{d}z}\exp(-iq_z z)\right|^2 \tag{4}$$

where R_F is the Fresnel reflectivity at an infinitely sharp interface and d*SLD*(*z*)/dz is the gradient of neutron scattering length density (SLD, SLD(*z*) = $\sum b_i n_i$, where b_i is the scattering length and n_i is the number density of atomic species i of the sample along the surface normal. Thus, by reflectivity measurement, it is possible to detect even a very small variation of the segregated polymer layers, which induce the SLD gradient to the *z*-direction. This contrast can be easily achieved due to the difference in the scattering length of the isotopes of hydrogen: $b_H = -3.74 \times 10^{-5}$ Å and $b_D = 6.67 \times 10^{-5}$ Å. The SLD values for D-PS block, PPrMA, and silicon are 6.42×10^{-6} Å^{-2}, $\sim 0.67 \times 10^{-6}$ Å^{-2}, and 2.07×10^{-6} Å^{-2}, respectively. We repeatedly scanned the reflectivity to monitor the formation of phase separated lamellar layers upon heating. To analyze the reflectivity data, the recursive Parratt formalism was used. The fitting multilayered modeling process can be found elsewhere.[38,39] We systematically varied and then optimized the fitting parameters such as SLD, interfacial roughness *s*, and layer thickness *d* until χ^2 (chi-square) error was minimized.

Results and Discussions

Phase Coherence in Compressible Diblock Copolymer Films. Our model system for compressible block copolymer films chosen here is deuterated polystyrene-*b*-poly(*n*-propyl methacrylate) (D-PS−PPrMA). These copolymers with molecular weights *M*s of 135 000, 119 600, and 75 300 exhibit LDOT of $\sim$190 and $\sim$225 °C and no ODT at 0.1 MPa, respectively.[40] For simplification purposes, the copolymers are taken to be perfectly monodisperse and symmetric. To characterize D-PS−PPrMA, various molecular parameters are required, which include ϵ_{ii}, σ_i, and N_i for pure polymers, and ϵ_{ij} for cross interaction between different polymers. Those parameters for the PS block are obtained from the best fit of the CS equation of state to volume data by Quach and Simha:[41] $\sigma_1 = 4.04$ Å, $h_z\epsilon_{11}/k = 4107.0$ K, and $N_1/M(\pi\sigma^3/6) = 0.41857$. The PPrMA block is characterized by $\sigma_2 = \sigma_1$, $h_z\epsilon_{22}/k = 3835.1$ K, and $N_2/M(\pi\sigma^3/6) = 0.41020$, which were determined from best fitting the equation of state to the volume data of PPrMA by Zoller[42] while fixing $\sigma_2 = \sigma_1$. The cross interaction ϵ_{ij} is interpreted as a kind of free energy to account for the weak directional interactions between the phenyl groups of the PS block and the ester groups of the PPrMA block, as was done in the previous analysis on the loop-forming D-PS-poly(*n*-pentyl methacryaltes) and the LDOT-type D-PS-poly(*n*-alkyl methacrylates) with ethyl to *n*-butyl side groups:[32,40] $\epsilon_{ij} \rightarrow \epsilon_{ij} + \delta\epsilon - kT\ln[\theta(1+\zeta)]$. Here, ϵ_{ij} represents the nonpolar cross interaction and $\delta\epsilon$ the energy increment due to the directional interactions. The ratio of the statistical degeneracies of nonpolar and directional interactions is denoted as ζ. This ratio is simply fixed to 11, implying that the specific interaction pair is formed only in the limited range of spatial arrangements of two dissimilar monomers. The symbol θ represents the fraction of the total number of cross-contacts that are directional, which satisfies the Boltzmann statistics as $\theta = [1 + \zeta\exp(-\delta\epsilon/kT)]^{-1}$. The bulk ODT data are used to determine ϵ_{12} ($= 0.98505(\epsilon_{11}\epsilon_{22})^{1/2}$) and $\delta\epsilon$ ($\delta\epsilon/k = 68$). The chosen set of molecular parameters yields the bulk LDOT of 180 and 226 °C for the copolymers with *M* of 135 000 ($N = 2693.2$) and 119 600 ($N = 2386.0$), respectively, which are in good agreement with the experimental values of 190 and 225 °C for those copolymers. No ordering is predicted for the copolymer with *M* of 75 300 ($N = 1502.2$),

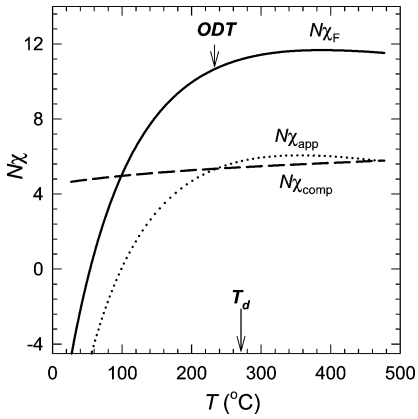

Figure 1. Effective Flory interaction parameter, $N\chi_F$, for D-PS−PPrMA with $M = 119\,600$ at ambient pressure plotted against temperature. In addition, $N\chi_{app}$ and $N\chi_{comp}$($N\chi_{app}+N\chi_{comp} = N\chi_F$) are drawn together.

as in the experiments. The directional interaction is considered to be the main source of the observed LDOT.

We first show the behavior of $N\chi_{app}$, $N\chi_{comp}$, and $N\chi_F$ for the copolymer with $M = 119\,600$ as a function of temperature at 0.1 MPa. The input directional interaction renders the system favorable in its energetics at lower temperatures: $N\chi_{app} < 0$ below ~100 °C, which then yields $N\chi_F < 0$ below ~50 °C. The demixing tendency gradually grows with the increase of temperature before reaching degradation temperature (T_d), as depicted in Figure 1. This behavior is caused by the fact that the entropic penalty to form directional interaction pairs is harder to overcome with more input of thermal energy, which is reflected by the behavior of $N\chi_{app}$. It is seen that $N\chi_{comp}$ is quite large because of the difference between self-interactions, $\epsilon_{11} > \epsilon_{22}$, and then $\partial P/\partial\phi$. This large $N\chi_{comp}$ is the source of baroplastic behavior of this copolymer, as the applied pressure increases B_T to yield the diminished $N\chi_{comp}$ and accordingly $N\chi_F$. It is predicted that the copolymer of $M = 135\,000$ reveals $dT_{LDOT}/dP \approx 104$ °C/100 MPa, while the experiments by Mayes and Russell give $dT_{LDOT}/dP \approx 90$ °C/100 MPa.[43]

Using the theory, the profiles formed in the copolymer film with certain external fields ($H_{\mp}$) acting at its surfaces can be simulated at temperatures prior to ODT, where the bulk copolymer melt is in the disordered state. The surface field parameter H_+ (or H_-) can better be described as the difference between substrate/A- and substrate/B-block interactions. The free surface is treated as a pseudo-substrate. Suppose for the copolymer of $M = 119\,600$ with $L/R_g = 14$ that tentative asymmetric surface fields preferential to the PPrMA block with $H_-/\epsilon_{PS} = -0.12$ and $H_+/\epsilon_{PS} = -0.01$ are acting on the substrate/polymer and the vacuum/polymer sides, respectively. These surface fields then produce first the surface segregation at 157 °C and 0.1 MPa shown in Figure 2a. As $H_{\mp}/\epsilon_{PS}$ values suggest, it is seen that the surface segregation on the right is weaker than that on the left. Such a tentative value of H_- is taken because of the affinity between silicon oxide and methacrylate blocks and so is H_+ because of the information on surface tension γ of the two blocks, where γ_{PPrMA} is slightly smaller than γ_{PS}. Raising the temperature to 215 °C for the same copolymer film makes the system reveal the phase coherent profile in Figure 2b, as the increased demixing tendency lets surface segregation propagate through the center of the film. At this thickness of L/R_g for the film, there were nine alternating lamellar layers formed including thinner ones adjacent to each surface. If symmetric surface fields with $H_{\mp}/\epsilon_{PS} = -0.12$ are taken, then the symmetrically decaying profiles from both surfaces are observed, as seen in Figure 2c. For comparison purposes, an antisymmetric situation is depicted in Figure 2d, where the surface fields are taken as $H_-/\epsilon_{PS} = -0.12$ and $H_+/\epsilon_{PS} = 0.12$. In this case, the film adjusts itself to revealing 10 alternating layers in order to accommodate the antisymmetric character.

In Figure 3, the theoretical decay length ξ of the surface segregated or phase coherent pattern of the copolymer films with three different Ms is plotted as a function of temperature at ambient pressure. The ξ is reduced to be dimensionless by multiplying it by the wave number q_0 of the equilibrium bulk profiles ($q_0 = \Omega(\bar{\chi} \rightarrow \bar{\chi}_s)$). It is re-emphasized that the phase demixing tendency is increased in this copolymer along with the increase of temperature because of the entropic penalty to form directional interactions. This procedure results in the increasing decay length with temperature. In the present mean-field picture, ξ diverges at the mean-field spinodals of the copolymer. As the decay length ξ is independent of the surface field parameter $H_{\mp}$, a direct comparison of theoretical ξ with experimental values is possible.[44]

Interpretation of Neutron Reflectivity Data. In Figure 4a, we plot neutron reflectivity results as a function of q_z for D-PS−PPrMA thin films with a molecular weight M of 119 600. The different curves correspond to different annealing temperatures as indicated in the figure. The solid lines together with the symbols are the best-fits obtained by the corresponding volume fraction profiles, which are shown in Figure 4b. A nine-layer model on a silicon substrate, representing a multilayered polymer thin film in an alternating sequence of two different polymer blocks, D-PS and PPrMA, **Si**(δ_{Si}, s_{Si})/**SiO**(δ_{SiO}, s_{SiO}, d_{SiO})/**P$_1$**(δ_{P1}, s_{P2}, d_{P3})/**P$_2$**(δ_{P2}, s_{P2}, d_{P2})/**P$_3$**(δ_{P3}, s_{P3}, d_{P3})/..... /**P$_8$**(δ_{P8}, s_{P8}, d_{P8})/**P$_9$**(δ_{P9}, s_{P9}, d_{P9})/vacuum was used, where δ is the scattering length density (SLD), s_J is the interfacial roughness, and d_J is the thickness for given layers. Note that an oxide layer (**SiO**) of 20 Å, adjacent to the **Si** substrate, is also taken into account, besides the polymer layers (**P**$_{1\sim9}$). During the fitting process, δ, s, and d of **P$_1$**, **P$_2$**, **P$_3$**, **P$_8$**, and **P$_9$** layers, which are close to an asymmetric medium (**P$_1$**, **P$_2$**, and **P$_3$** for SiO surface and **P$_8$** and **P$_9$** for vacuum) were independently floated, in order to include the structural abnormalities which might be induced by the presence of boundary surfaces. On the other hand, s and d of **P$_4$** and **P$_5$** were constrained with **P$_6$** and **P$_7$**, respectively, in order to simulate the periodic nature of the lamella layering system. As noted earlier, all the layers were considered as independent and possessing a certain interface profile. When the interfacial roughness is larger than the thickness of its underlying layer ($s_J > d_J$), the total density profile can produce a *discontinuous* model profile, which is not realistic in nature. In order to generate continuous total model profiles from the multilayers (**P$_1$**~**P$_9$**) as shown in Figure 4b, we employed the effective-density calculation, instead of the classical box model.[45] In this method, we first guess the whole profile, $\delta(z)$ with the hyperbolic tangent function for each interface, and then each layer profile is sliced into very thin layers (~1 Å thickness) with uniform dispersions and sharp interfaces.[46] Therefore, the reflectivity could be calculated using the Parratt formalism.

At $T = 50$ °C ($T \ll T_{LDOT}$), the reflectivity spectrum exhibits a single periodic oscillation corresponding to total film thickness, approximately, $d = 2\pi/\Delta q_z \sim 1200$ Å, indicating that D-PS and PPrMA blocks are not phase-separated, when it was spin-coated on a silicon wafer. Along with the single periodic oscillation, the fitting results indicate that a partially segregated PPrMA layer (**P$_1$**) with $d_{P1} = 72$ Å exists near the SiO surface. In close proximity to the segregated PPrMA layer on the SiO surface, its counterpart block, D-PS forms a 123 Å thick layer

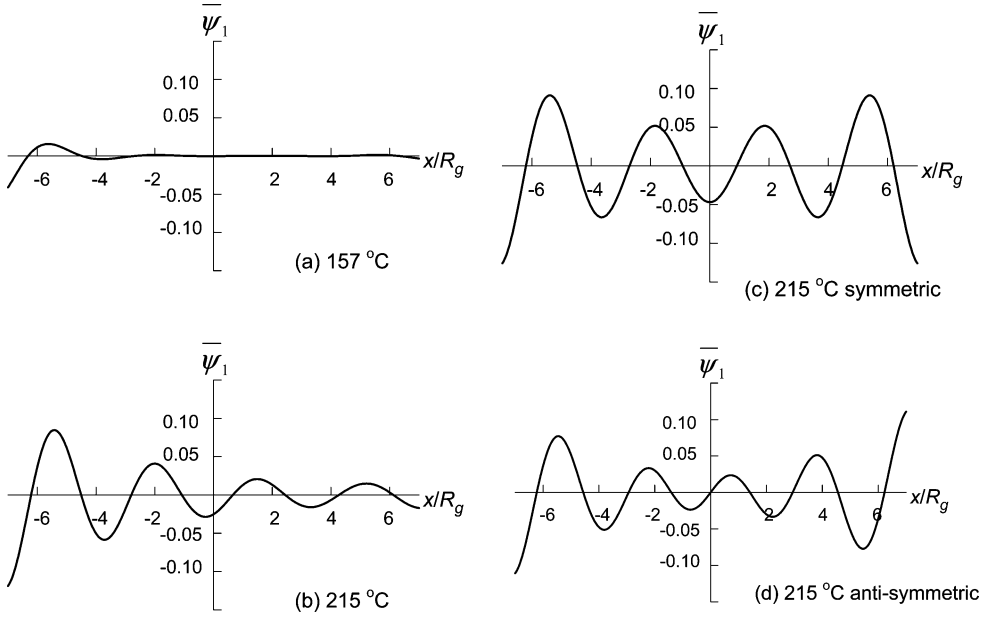

Figure 2. Optimized profiles of lamella-forming D-PS−PPrMA copolymer film at (a) 157 and (b−d) 215 °C as a function of film thickness x/R_g. The surface fields are chosen as (a,b) $H_-/\epsilon_{PS} = -0.12$ at the substrate/polymer surface ($x = -L/2$) and $H_+/\epsilon_{PS} = -0.01$ at vacuum/polymer surface ($x = +L/2$), where both surfaces attract PPrMA block; (c) $H_-/\epsilon_{PS} = -0.12$ and $H_+/\epsilon_{PS} = -0.12$ (symmetric case); (d) $H_-/\epsilon_{PS} = -0.12$ and $H_+/\epsilon_{PS} = 0.12$ (antisymmetric case).

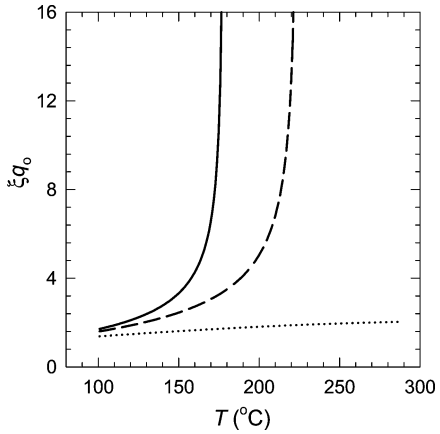

Figure 3. Theoretical decay length ξq_0 for D-PS−PPrMA copolymers, where q_0 denotes the wave number of the equilibrium bulk profiles. The molecular weight M of the samples is 135 000 (—), 119 600 (− − −), and 75 300 (·· ··), respectively.

($\mathbf{P_2}$), yielding a higher SLD increment of 5.24×10^{-6} Å^{-2}, corresponding to $\phi_{P2} = 0.80$ of the pure D-PS layer. This oscillation in the total SLD profile was damped rapidly away from the surface, and any other characteristic feature was not observed into the film. This type of early segregation is similar to the one used by Mansky et al. for D-PS-*b*-poly(*n*-butyl methacrylate)[16] and Menelle et al. for PS-*b*-deuterated poly(methyl methacrylate) thin layers.[8] This surface enrichment of the PPrMA segments was explained as being due to stronger attractive interactions between the PrMA segments and the SiO substrate, as theoretically shown in Figure 2a. On the other hand, no visible surface ordering was observed at the vacuum/polymer surface but a fairly rough surface with $s_{P9} \sim 54$ Å indicates that tiny topographical structures (islands or terrace) might be present. The NR spectrum and SLD profiles then remain fairly constant up to $T \sim 157$ °C, while the surface roughness (s_{P9}) at the vacuum/polymer is observed to increase slightly.

As T approaches the bulk T_{LDOT} (~225 °C) of D-PS−PPrMA, the oscillation in the SLD profile initiated from the substrate propagates into the film. Simultaneously a sudden SLD increase at the vacuum/polymer interface in the SLD profile for $T =$ 171 °C is observed, indicating the onset of island formation. The onset of island formation can be further confirmed by the observation of reflectivity below the critical edge, as discussed elsewhere.[14] In fact, a significant reduction (dashed line in Figure 4a) in the reflectivities at the critical edge was found, when temperatures were higher than 171 °C. A distinct first-order Bragg peak suddenly appeared at $q_z \sim 0.0224$ Å^{-1} between 171 and 187 °C, indicative of the onset of the phase matching. As temperature increases further to 200 °C (still below the bulk T_{LDOT}), the second-order Bragg reflection at $q_z \sim 0.0368$ Å^{-1} is also visible, and the intensity of the first-order Bragg reflection becomes as high as one at the critical q_z. At $T = 215$ °C, the third-order Bragg reflection at $q_z \sim 0.0550$ Å^{-1} is now apparent, and no further noticeable change in NR spectrum was observed at $T > 215$ °C. Note that, in order to test whether each reflectivity at all temperatures represents a kinetically stable structure, we scanned the reflectivity twice at the same temperature, and two reflectivity curves at the same temperature exactly matched each other, indicating that the spatial transformation of the polymers is not dependent on time but on temperature.

At $T = 187$ °C, a clear oscillation in the SLD profile, coherently propagated through the entire film thickness, reaches up to the vacuum/polymer surface. From Figure 4b, one can also see that the first oscillation from the vacuum contacting layer gets abruptly shifted to higher z, indicative of a sudden increase of the total film thickness. These phenomena can be rationalized as the result of rapid evolution of the islands formation and coarsening process due to the phase mismatch (characterized by the total film thickness/the phase spacing) when the transition is propagated from the layer adjacent to SiO. Because of this structural deformation at the polymer/vacuum surface, it was difficult to determine whether there was a similar contribution of the phase correlation into the film as at the polymer/SiO surface.

The overall qualitative features shown by the experimental profiles in Figure 4 are in fair agreement with the simulated ones in Figure 2a,b for the copolymer film with asymmetric

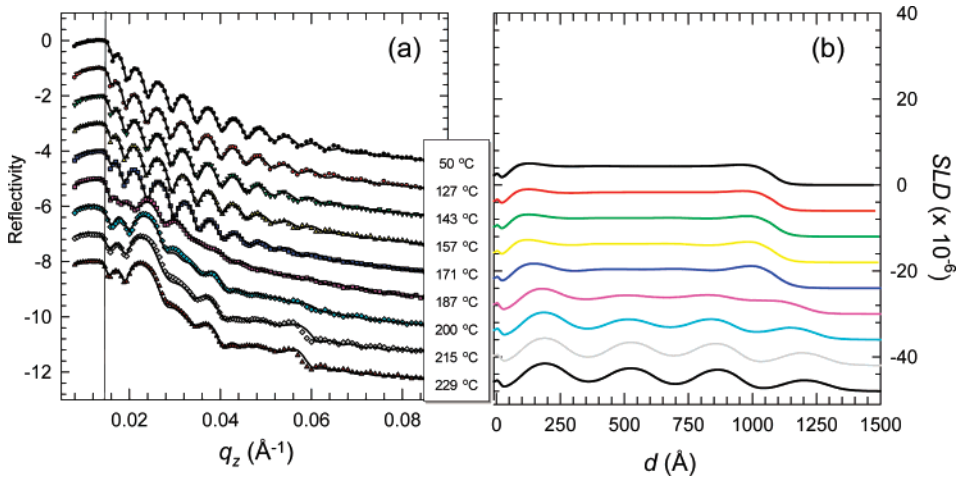

Figure 4. (a) Neutron reflectivity data (symbols) of D-PS−PPrMA films with $M = 119\,600$ at various temperatures. The solid lines through the data are the best fits. The curves are shifted arbitrarily for clarity. (b) The corresponding SLD profiles are obtained from the fits of part a. The *x*-axis, *d*, is taken from the substrate.

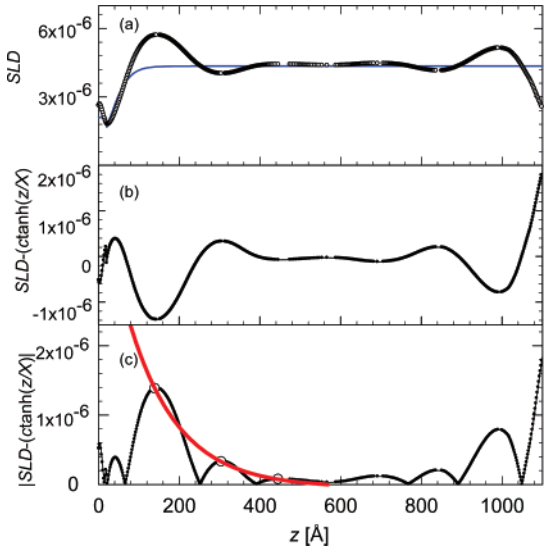

Figure 5. (a) SLD profile (○) of D-PS−PPrMA films at $T = 171$ °C with a hyperbolic tangent fit (line). (b) The hyperbolic tangent has been subtracted. (c) The symbols are obtained from the absolute value of part b, and the maxima of the first three peaks from the substrate are fitted with a decay function of $e^{-z/\xi}$ (line).

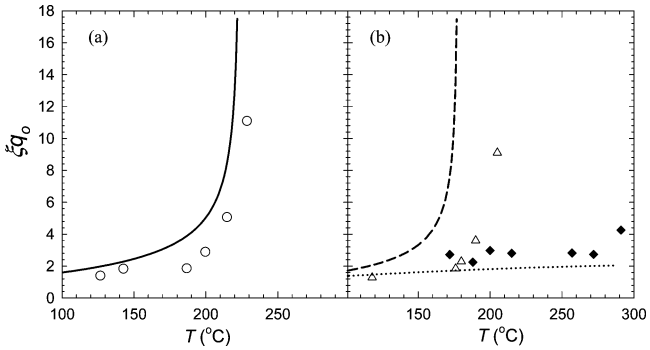

Figure 6. Comparison of the experimental ξq_0, obtained from the previous figure, with the theoretical one. The molecular weight *M* of the samples is 119 600 (○ in plot a), 135 000 (△ in part b), and 75 300 (♦ in part b), respectively.

surface fields ($|H_-| \gg |H_+|$). A more vivid comparison of theory and experiment can be made as follows. The extent of propagation in the oscillation in the SLD profile can be characterized by decay length ξ. Since we used the nine independent layered model to generate the SLD profiles, instead of the formulated functional form with ξ and *z* that appeared in many published papers,[7,8] the decay length scale was estimated as it appeared in ref 47. In details, the symbols in Figure 5a show an example of a SLD profile, SLD_{exptl}, at $T = 171$ °C obtained by the best-fitting. Then, the SLD profile (line in Figure 5a) was fitted by a hyperbolic tangent function, $SLD(z) = SLD_o + SLD_1 \tanh(z/X)$, in order to visualize the oscillation pattern more clearly in the SLD profile. The fitted SLD profile, SLD(*z*), represents a SLD profile with no phase separation. Then the fitted line was subtracted from the experimental data, given by, $\Delta SLD = SLD_{exptl} - SLD(z)$, which is shown in Figure 5b. Note that the phase coherence in ΔSLD and its decaying nature into the thin film are more easily visible. To obtain the decay length ξ of ΔSLD, the absolute value of the SLD density profile was generated as shown in Figure 5c, and peaks in the profile were identified. An exponential function, $e^{-z/\xi}$ was used to fit to the maxima of the peaks (narrow line in Figure 5c), from which the decay length was calculated. When temperatures were much below T_{LDOT}, the decay lengths increased slightly but progressively with temperature. As *T* approached T_{LDOT}, the decay lengths became longer and increased rapidly. This situation is depicted in Figure 6a, where ○ show ξ values at the indicated temperature for the D-PS−PPrMA films with molecular weight *M* of 119 600. In order to compare these experimental results with the theoretical ones described earlier, ξ was multiplied with the characteristic wave number q_0, obtained from the Bragg peaks of the NR. The q_0 reads 0.0169 Å^{-1} for the copolymer.[48] In this plot, the theoretically evaluated ξq_0 from Figure 3 is shown together with the experimentally deduced values. It is seen that theory and experiment are in good agreement. However, the experimental ξq_0 does not show divergence around the bulk ordering temperature, as is the case for the variational method suggested by Tang and Freed.[10]

The same analysis was applied to the NR data for D-PS−PPrMA thin films with molecular weights *M*s of 135 000 (see Supporting Information) and 75 300 (see Supporting Information). To compare these experimental results with the theoretical ones, ξ was again multiplied by the wave number q_0, obtained from the Bragg peaks of the NR, and then plotted against temperature as seen in Figure 6b. The characteristic wave number q_0 reads 0.0147 and 0.0217 Å^{-1} for the copolymer of $M = 135\,000$ and 75 300, respectively.[48] The general trends of ξq_0 for the polymers with different molecular weights were found to be in accord with the theoretical lines drawn together.

In summary, we have investigated a mean-field Landau analysis on block copolymer films exhibiting ordering upon heating due to directional interactions and compressibility. There are certain limitations of the present theory. It is only applicable to the weak segregation regime. The free energy functional was only obtained for lamellae and the Euler−Lagrange equation was solved in a linearized fashion. A variation calculation can be introduced to add the nonlinear contributions. The resultant decay length is divergent at spinodals in this linearized solution. It is quite remarkable that the present mean-field analysis, despite its limitations, gives a molecular interpretation and semiquantitative predictability of phase coherence upon heating and the resultant decay lengths, which were tested with the neutron reflectivity measurements and the subsequent interpretation of the reflectivity data. As we demonstrate here, molecular information can be put into theory through χ_F from the compressible RPA. The recent Landau free energy developed by Angerman et al.[13] for various nanopatterned block copolymer films can be generalized to contain molecular information in a similar way. It is also possible that a self-consistent field approach may be devised in connection with the effective RPA interactions for a compressible block copolymer system to go beyond the weak segregation regime. The air-contact surface may be treated in a self-consistent way in these compressible systems. In addition, the theory is capable of predicting pressure effects on phase coherence behavior in block copolymer films. These prospects are the subject of future studies.

Concluding Remarks

Phase coherence behavior upon heating in compressible diblock copolymer films has been studied for the control and design of nanopatterned films in a vast processing window. An effective Landau free energy from a compressible random-phase approximation (RPA) approach was manipulated to obtain a real-space free energy functional for the copolymer films with surface−monomer interactions acting as an external field. The minimization of the free energy functional, which was first linearized in the weak segregation regime, yielded the profiles and decay lengths of surface segregated or phase coherent copolymer films. Taking thin films of deuterated polystyrene-*b*-poly(*n*-propyl methacrylate) (D-PS−PPrMA) as a model system, neutron reflectivity measurements were performed to compare the theoretical profiles and decay lengths with the experimental ones. D-PS−PPrMA, which exhibits ordering upon heating and its suppression under applied pressure in the bulk state due to weak directional interactions and a finite compressibility difference between constituent monomers, develops phase coherent profiles growing with temperature and then decay lengths from them. The chosen molecular parameters that characterize the copolymer in the bulk state are shown to yield the predicted decay length ξ in accord with the experimental values except that this mean-field theory reveals divergence of ξ at spinodal temperatures.

Acknowledgment. This work has been supported by the Nuclear Research and Development Program (Grant M20602000060-06B0200-06010) from Korea Science and Engineering Foundation (KOSEF). J.C. also acknowledges the financial support from Hyperstructured Organic Materials Research Center funded by KOSEF, and K.S. acknowledges the financial support from Center for Nanostructured Materials Technology under 21st Century Frontier R&D Program (Grant 06K1501-01311) and KAIST-BAERI of the Ministry of Science and Technology, Korea. J.K.K. acknowledges the National Creative Research Initiative Program supported by KOSEF. Neutron reflectivity was performed at HANARO supported by KAERI, Korea, and at NIST, U.S. Department of Commerce.

Appendix

Solution of the Euler−Lagrange Equation for Block Copolymer Films. The real-space version of the free energy functional in eq 1 for lamellae-forming compressible block copolymer films after Ohta−Kawasaki treatment yields the Euler−Lagrange equation as

$$A\int_{-L/2}^{L/2} G(x-x')\bar{\psi}_1(x')\mathrm{d}x' - B\frac{\mathrm{d}^2\bar{\psi}_1}{\mathrm{d}x^2} - \bar{\chi}\bar{\psi}_1 + \frac{\mu}{2!}\bar{\psi}_1^{\,2} + \frac{\lambda}{3!}\bar{\psi}_1^{\,3} - \theta = 0 \quad \text{(A1)}$$

with the boundary conditions as follows

$$-\beta H_{\pm} \pm B\frac{\mathrm{d}\bar{\psi}_1}{\mathrm{d}x}|_{x=\pm L/2} = 0 \quad \text{(A2)}$$

In eq A1, $G(x)$ means the Green function for chain connectivity, and the two symbols μ and λ, respectively, denote the vertex functions in eq 1 under the conventional local approximation. We choose the simplest form of the Green function as

$$G(x-x') = \begin{cases} x-x' & (x > x') \\ 0 & (x < x') \end{cases} \quad \text{(A3)}$$

The linearized solution of the given Euler−Lagrange equation can then be obtained as

$$\bar{\psi}_1(x) = \mathrm{e}^{x/\xi}(D_{c+}\cos\Omega x + D_{s+}\sin\Omega x) + \mathrm{e}^{-x/\xi}(D_{c-}\cos\Omega x + D_{s-}\sin\Omega x) \quad \text{(A4)}$$

where a transformation of $x + L/2 \rightarrow x$ has been done in eq A4. The four coefficients of eq A4 can be given from three unknowns, $\bar{\psi}_1(0)$, $\bar{\psi}_1'(0)$, and θ, as

$$D_{c\pm} = \frac{1}{2}\left[\bar{\psi}_1(0) \pm \frac{\xi\Omega}{2}\bar{\psi}_1'(0)\right]; \quad D_{s\pm} = \frac{\bar{\psi}_1'(0)}{4} \mp \frac{\xi\theta}{4B\Omega} \mp \frac{1}{2\xi\Omega}\left(\frac{\xi^2\bar{\chi}_S}{4B} - 1\right)\bar{\psi}_1(0) \quad \text{(A5)}$$

After applying the two boundary conditions and the material balance equation, θ is first obtained as $\xi\theta/4B\Omega = (1/2)K_1\bar{\psi}_1(0) + (1/4)K_2\psi_1'(0)$, where K_1 and K_2 are given by

$$K_1 \equiv \frac{f_{c+} - f_{c-} + (f_{s+} - f_{s-})(\xi^2\bar{\chi}_s/4B - 1)/\xi\Omega}{f_{s-} - f_{s+}}; \quad K_2 \equiv \frac{\xi\Omega(f_{c+} + f_{c-}) - (f_{s+} + f_{s-})}{(f_{s-} - f_{s+})} \quad \text{(A6)}$$

The newly appearing f's in eq A6 are given from the limiting values of $\bar{\psi}_1$ at $x = L$ as

$$f_{c\pm} \equiv \mathrm{e}^{\pm L/\xi}(1/\xi\Omega\cos\Omega L \pm \sin\Omega L); \quad f_{s\pm} \equiv \mathrm{e}^{\pm L/\xi}(\cos\Omega L \mp 1/\xi\Omega\sin\Omega L) \quad \text{(A7)}$$

It can be shown that $\bar{\psi}_1'(0) = -H_-/B\Omega$. Finally, $\bar{\psi}_1(0)$ can be written as

$$\bar{\psi}_1(0) = \frac{\beta H_+/B\Omega - (\gamma_{c+}\tau_{c+} + \gamma_{s+}\tau_{s+} + \gamma_{c-}\tau_{c-} + \gamma_{s-}\tau_{s-})}{\gamma_{c+}\alpha_{c+} + \gamma_{s+}\alpha_{s+} + \gamma_{c-}\alpha_{c-} + \gamma_{s-}\alpha_{s-}} \quad \text{(A8)}$$

where each term appearing in this equation is as follows

$$\alpha_{c\pm} = \frac{1}{2}; \quad \alpha_{s\pm} = \frac{\mp(\xi^2\bar{\chi}_s/4B - 1)/\xi\Omega \mp K_1}{2}$$

$$\tau_{c\pm} = \mp\frac{\beta H_-/B\Omega}{4/\xi\Omega}; \quad \tau_{s\pm} = -\frac{1 \mp K_2}{4} \times \frac{\beta H_-}{B\Omega}$$

$$\gamma_{c\pm} = \pm f_{c\mp}\, e^{\pm 2L/\xi}; \quad \gamma_{s\pm} = f_{s\mp}\, e^{\pm 2L/\xi} \tag{A9}$$

As a final comment, eq A4 can be used for a variational calculation to include the nonlinear effects on the free energy functional, as was done by Tang and Freed.[10] Their findings such as finite decaying lengths at spinodals are expected to be reproduced.

Supporting Information Available: Neutron Reflectivity data of D-PS−PPrMA films with $M = 135\,000$ and 75 300 and their corresponding SLD profiles. This material is available free of charge via the Internet at http://pubs.acs.org.

References and Notes

(1) Hamley, I. W. *The Physics of Block Copolymers*; Oxford University Press, Inc.: New York, 1998.
(2) Hadjichristidis, N.; Pispas, S.; Floudas, G. A. *Block Copolymers: Synthetic Strategies, Physical Properties, and Applications*; John Wiley & Sons, Inc.: Hoboken, NJ, 2003.
(3) Hamley, I. W., Ed. *Developments in Block Copolymer Science and Technology*; John Wiley & Sons Ltd.: Chichester, U.K., 2004.
(4) Leibler, L. *Macromolecules* **1980**, *13*, 1602.
(5) Ohta, T.; Kawasaki, K. *Macromolecules* **1986**, *19*, 2621.
(6) Binder, K. In *Polymers in Confined Environments*; Granick, S., Ed.; Springer-Verlag: Berlin, Germany,1999.
(7) Anastasiadis, S. H.; Russell, T. P.; Satija, S. K.; Majkrzak, C. F. *Phys. Rev. Lett.* **1989**, *62*, 1852.
(8) Menelle, A.; Russell, T. P.; Anastasiadis, S. H.; Satija, S. K.; Majkrzak, C. F. *Phys. Rev. Lett.* **1992**, *68*, 67.
(9) Fredrickson, G. H. *Macromolecules* **1987**, *20*, 2535.
(10) Tang, H.; Freed, K. F. *J. Chem. Phys.* **1992**, *97*, 4496.
(11) Fredrickson, G. H.; Ganesan, V.; Drolet, F. *Macromolecules* **2002**, *35*, 16.
(12) Fredrickson, G. H. *The Equilibrium Theory of Inhomogeneous Polymers*; Oxford University Press: Oxford, U.K., 2006.
(13) Angerman, H. J.; Johner, A.; Semenov, A. N. *Macromolecules* **2006**, *39*, 6210.
(14) Russell, T. P.; Karis, T. E.; Gallot, Y.; Mayes, A. M. *Nature* **1994**, *386*, 729.
(15) Ruzette, A.-V. G.; Banerjee, P.; Mayes, A. M.; Pollard, M.; Russell, T. P.; Jerome, R.; Slawecki, T.; Hjelm, R.; Thiyagarajan, P. *Macromolecules* **1998**, *31*, 8509.
(16) Mansky, P.; Tsui, O. K. C.; Russell, T. P.; Gallot, Y. *Macromolecules* **1999**, *32*, 4832.
(17) Kim, E. Y.; Lee, D. J.; Kim, J. K.; Cho, J. *Macromolecules* **2006**, *39*, 8747.
(18) Pollard, M.; Russell, T. P.; Ruzette, A.-V.; Mayes, A. M.; Gallot, Y. *Macromolecules* **1998**, *31*, 6493.
(19) Ruzette, A.-V.; Mayes, A. M.; Pollard, M.; Russell, T. P.; Hammouda, B. *Macromolecules* **2003**, *36*, 3351.
(20) Ryu, D. Y.; Lee, D. H.; Kim, J. K.; Lavery, K. A.; Russell, T. P.; Han, Y. S.; Seong, B. S.; Lee, C. H.; Thiyagarajan, P. *Phys. Rev. Lett.* **2003**, *90*, 235501.
(21) Gonzalez-Leon, J. A.; Acar, M. H.; Ryu, S. W.; Ruzette, A.-V.; Mayes, A. M. *Nature* **2003**, *426*, 424.
(22) Gonzalez-Leon, J. A.; Ryu, S. W.; Hewlett, S. A.; Ibrahim, S. H.; Mayes, A. M. *Macromolecules* **2005**, *38*, 8036.
(23) Lavery, K. A.; Sievert, J. D.; Watkins, J. J.; Russell, T. P.; Ryu, D. Y.; Kim, J. K. *Macromolecules* **2006**, *39*, 6580.
(24) Ryu, D. Y.; Jeong, U.; Kim, J. K.; Russell, T. P. *Nature Mater.* **2002**, *1*, 114.
(25) Ryu, D. Y.; Lee, D. H.; Jeong, U.; Yun, S.-H.; Park, S.; Kwon, K.; Sohn, B.-H.; Chang, T.; Kim, J. K.; Russell, T. P. *Macromolecules* **2004**, *37*, 3717.
(26) Li, C.; Lee, D. H.; Kim, J. K.; Ryu, D. Y.; Russell, T. P. *Macromolecules* **2006**, *39*, 5926.
(27) Dudowicz, J.; Freed, K. F. *Macromolecules* **2000**, *33*, 5292.
(28) Ruzette, A.-V.; Banerjee, P.; Mayes, A. M. *J. Chem. Phys.* **2001**, *114*, 8205.
(29) Ruzette, A.-V.; Mayes, A. M. *Macromolecules* **2001**, *34*, 1894.
(30) Cho, J. *Macromolecules* **2001**, *34*, 1001.
(31) Cho, J. *J. Chem. Phys.* **2003**, *119*, 5711.
(32) Cho, J. *Macromolecules* **2004**, *37*, 10101.
(33) Cho, J.; Wang, Z.-G. *Macromolecules* **2006**, *39*, 4576.
(34) Cho, J. *Polymer* **2007**, *48*, 429.
(35) Cho, J.; Sanchez, I. C. *Macromolecules* **1998**, *31*, 6650.
(36) Cho, J. *Macromolecules* **2000**, *33*, 2228.
(37) Shin, K.; Hu, X.; Zheng, X.; Rafailovich, M. H.; Sokolov, J.; Zaitsev, V.; Schwarz, S. A. *Macromolecules* **2001**, *34*, 4993.
(38) Li, J.; Zhao, W.; Quinn, J.; Rafailovich, M. H.; Sokolov, J.; Lennox, R. B.; Eisenberg, A.; Wu, X. Z.; Kim, M. W.; Sinha, S. K.; Tolan, M. *Langmuir* **1995**, *11*, 1785.
(39) Shin, K.; Rafailovich, M. H.; Sokolov, J.; Chang, D. M.; Cox, J. K.; Lennox, R. B.; Eisenberg, A.; Gibaud, A.; Huang, J.; Hsu, S. L.; Satija, S. K. *Langmuir* **2001**, *17*, 4955.
(40) These transition temperatures for D-PS−PPrMA are obtained from the recent small-angle neutron scattering measurements on the homologous series of D-PS-Poly(*n*-alkyl methacrylates). See: Ryu, D. Y.; Shin, C.; Cho, J.; Lee, D. H.; Kim, J. K.; Lavery, K. A.; Russell, T. P. *Macromolecules* **2007**, *40*, 7644.
(41) Quach, A.; Simha, R. *J. Appl. Phys.* **1971**, *42*, 4592.
(42) Zoller, P.; Walsh, D. *Standard Pressure-Volume-Temperature Data for Polymers*; Technomic Publishing Co., Inc.: Lancaster, PA, 1995.
(43) To obtain dT_{LDOT}/dP, Mayes and Russell attempted the superposition of scattering intensity curves for hydrogeneous PS−PPrMA at various pressures. See: Ruzette, A.-V. G.; Banerjee, P.; Mayes, A. M.; Pollard, M.; Russell, T. P.; Jerome, R.; Slawecki, T.; Hjelm, R.; Thiyagarajan, P. *Macromolecules* **1998**, *31*, 8509. Recently, we have performed the direct measurements of LDOT at elevated pressures to find $dT_{LDOT}/dP \approx 63$ °C/100 MPa. The Hartree (fluctuation correction) analysis developed for compressible block copolymers theory yields this coefficient of ~76 °C/100 MPa, which is somewhat smaller than the present mean-field result. See the note in ref. 40.
(44) The present theory allows system compressibility. Thus, the effects of pressure on the profiles of the film can also be analyzed with the theory. From Figure 1, it is predicted that pressurization of the copolymer film suppresses the phase coherence because of the baroplastic character of the copolymer. A quick calculation yields that D-PS−PPrMA films with $M = 119\,600$ at 215 °C has the decay length ξ at 50 MPa 4 times smaller than that at ambient pressure.
(45) Tolan, M. *X-ray Scattering from Soft-Matter Thin Films*; Springer-Verlag: Berlin, Germany, 1999.
(46) Russell, T. P. *Mater. Sci. Rep.* **1990**, *5*, 171.
(47) Saxena, R.; Bale, S. D.; Horbury, T. S. *Phys. Plasmas* **2005**, *12*, 052904.
(48) q_0 is obtained from the average of the differences between the three Bragg peaks, as suggested in ref 7. In case of the copolymer with $M = 75\,300$, only the first peak appears at 291 °C after 8 h of annealing.

MA071604R